

Design and Performance of 1762 nm Tm-doped Fiber Amplifiers for Manipulation and Control of Optical Qubits in $^{133}\text{Ba}^+$ Ions

Robert E. Tench, Adrian Zepeda, Wiktor Walasik, Alexandre Amavigan, and Jean-Marc Delavaux

Cybel LLC, 62 Highland Avenue, Bethlehem, PA 18017 USA

robert.tench@cybel-llc.com

Abstract—We report the optical architecture, experimental performance, and simulated performance of polarization- maintaining CW and pulsed single clad Tm-doped fiber amplifiers designed to operate over a wavelength span of 1760—1960 nm. We highlight the potential applications of these amplifiers to quantum computing and quantum qubit experiments using 1762 nm light. Our amplifier exhibits 3 W CW output power and 20 W peak pulsed output power (2 MHz rep. rate, 10% duty cycle) at 1762 nm. Measurements of the wavelength response of the TDFA yield an experimental operating bandwidth extending from < 1750 nm to > 1920 nm. Simulations of the amplifier bandwidth indicate a 3 dB (50% FWHM) wavelength span of 1745 nm to 1980 nm (135 nm). Experimental output power and bandwidth results agree well with the simulations. The external noise figure for this amplifier ranges from 7.5 dB to 9.5 dB. No linewidth broadening was observed in a typical TDFA output when using a single frequency input laser source with a linewidth of 10 kHz. We discuss suitability and applications of the TDFA to 1762 nm enabled manipulation of optical qubits in trapped $^{133}\text{Ba}^+$ ions.

Keywords—Fiber amplifier, infrared, polarization-maintaining, Thulium, 1762 nm, optical qubit shelving, optical qubit control, optical qubit manipulation, $^{133}\text{Ba}^+$, $^{138}\text{Ba}^+$.

I. INTRODUCTION

Over the past decade, much research has been done on quantum computing and state preparation and measurement (SPAM) in $^{88}\text{Sr}^+$, $^{43}\text{Ca}^+$, and $^{171}\text{Yb}^+$ ions for manipulation and control of qubits [1-6]. Recently a new ion, $^{133}\text{Ba}^+$, has been proposed for quantum computing, SPAM, and optical qubit manipulation, and many early successful experiments have been conducted [7- 14]. These experiments in the shelving, control, and manipulation of optical qubits in trapped Ba^+ ions rely on transitions between the $6^2\text{S}_{1/2}$ ground state and the $6^2\text{P}_{1/2}$ and $6^2\text{P}_{3/2}$ excited states (455 nm

and 493 nm), and between these three states and the $5^2\text{D}_{3/2}$ and $5^2\text{D}_{5/2}$ levels (585 nm, 614 nm, 650 nm, 1762 nm, and 2051 nm). Figure 1 shows these transitions schematically in a level diagram including laser wavelengths and level lifetimes. [15,16]

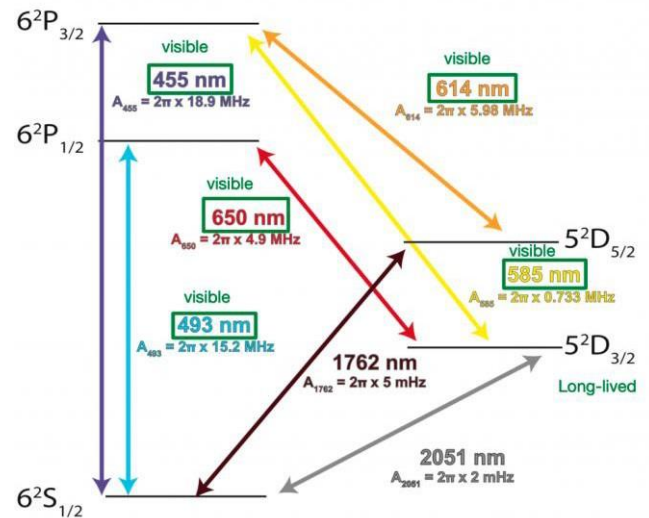


Figure 1. Gross $^{133}\text{Ba}^+$ energy level diagram with transition wavelengths and level lifetimes.

For quantum experimentalists, the generation of Watt-level single frequency laser radiation at the visible wavelengths in Figure 1 is relatively straightforward, and many attractive alternatives exist for these narrow linewidth sources. But most of the existing narrow linewidth, single frequency infrared laser sources at 1762 nm currently exhibit output powers of only 3- 100 mW [17-19], with the highest CW power so far reported of

only 500 mW [20]. As in atomic and molecular spectroscopy, higher laser output power is always better, and multi-watt sources are always more useful than milliwatt sources for improving the scalability with power, accuracy, and precision of existing quantum computing experiments as well as stimulating the development of future experiments and radical new technologies.

Therefore, a definite need exists for research on and development of narrow linewidth, single frequency multi-watt sources at 1762 nm and 2051 nm.

In this paper we report a 3 W CW Tm-doped fiber amplifier suitable for integration into existing optical qubit experiments using $^{133}\text{Ba}^+$ ions. The paper is organized as follows: Section II presents an introduction to the basic technology and current scope of fiber optical amplifiers in 2023 and illustrates the fundamental principles behind the operation of a Tm-doped fiber amplifier. Section III describes the optical architecture, design, and performance of 2–3W polarization-maintaining two-stage TDFAs designed for the 1760–1960 nm spectral region. Section IV covers the applications and integration of a 3W PM fiber amplifier into existing optical qubit experiments at 1762 nm, emphasizing the unique qualities of the TDFA that make it extremely useful and relevant for shelving, control, and manipulation of optical qubits. A discussion and conclusion are given in Section V.

II. BASICS OF FIBER AMPLIFIERS IN 2023 AND EXAMPLE OF A TDFA DESIGN

A. Survey of the State of Fiber Amplifiers in 2024

The first practical packaged semiconductor-laser-pumped Erbium-doped fiber amplifier, operating near 1550 nm, was introduced and demonstrated in August 1989 [21,22]. Since that time, tremendous progress has been made in the development of rare-earth-doped fiber amplifiers in many different infrared wavelength bands. Figure 2 summarizes the wavelength bands covered by current packaged fiber amplifiers, using Yb^{3+} , Bi^{3+} , Er^{3+} , Tm^{3+} , and Ho^{3+} as dopants in the cores of the single mode Si-based host fibers [23]. Note that the Tm- and Ho-doped fiber amplifiers cover a wide wavelength range of 1680–2130 nm. We will concentrate from this point forward on the performance of Tm-doped fiber amplifiers that readily access the important line in Ba^+ of 1762 nm.

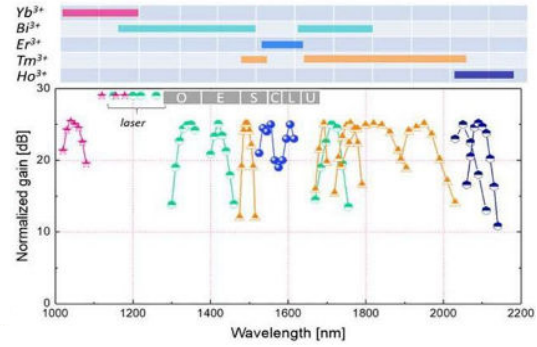


Figure 2. Graphical summary of the infrared wavelength bands covered by single clad doped fiber amplifiers in 2023.

Current Tm-doped single mode fiber optical amplifiers take a wavelength appropriate (e.g., 1760–1960 nm) low power infrared optical signal as an input, and greatly amplify this low power to a much higher optical power at the output. Both CW and pulsed signals can successfully be amplified. Typical values of input signals P_{in} are 1 mW–10 mW (0 dBm to 10 dBm), and typical output signals P_{out} are 0.5 W–5 W (+27 dBm to +37 dBm). Corresponding values of gain (P_{out}/P_{in}) are 17 dB to 37 dB.

Along with the process of optical amplification, which takes place through stimulated emission, there is the unavoidable addition of noise from the accompanying process of spontaneous emission. The noise contribution of a fiber amplifier is characterized by a noise figure (NF) which is defined as $10\log_{10}(\text{Input OSNR}/\text{Output OSNR})$ [24, 25] and is typically 5-10 dB for a fiber coupled device. OSNR is the optical signal-to-noise-ratio of the lightwave signals. The minimum quantum limited NF for a high gain fiber amplifier is 3.0 dB. [24, 25]

B. Example of a Simple TDFA Design

Every practical fiber coupled TDFA requires five essential components:

- 1) A length of single mode silica fiber doped with Tm^{3+} ions diffused in the core;
- 2) A source of pump light, absorbed at an appropriate low wavelength, that generates optical gain in a band of higher wavelengths through the process of stimulated emission;
- 3) A means of multiplexing the pump light and signal light together in the Tm-doped fiber;

- 4) Optical isolators to couple the input signal into the TDF, couple the output signal out of the TDF after amplification, establish unidirectional amplification, and minimize the effects of external reflections; and
- 5) Input and output fiber pigtails to interface the TDFA with the outside world.

All of these elements are present in the simple single stage TDFA shown schematically in Figure 3. Here an input signal from 1760-1960 nm passes through the connectorized input fiber and input isolator ISO1, and is coupled into the Tm-doped fiber. Pump light at 1567 nm is also coupled into the Tm-doped fiber through wavelength division multiplexer WDM1. At the output of the doped fiber, the amplified signal passes through WDM1 and output isolator ISO2 and is coupled out through the connectorized output fiber.

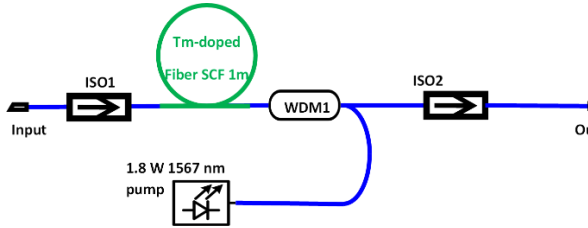


Figure 3. Optical architecture of a single stage Tm-doped fiber amplifier.

To quantitatively understand and model the performance of the TDFA, we first require a full knowledge of the wavelength-dependent gain and absorption coefficients of the Tm-doped fiber [24, 25]. Figure 4 plots the gain and absorption coefficients in dB/m vs. wavelength for the specific polarization-maintaining Tm-doped fiber used in the single stage TDFA [26, 27]. In this fiber, the absorption coefficient peaks near 1620 nm, and the gain coefficient peaks around 1800 nm. We note that the FWHM of the gain coefficient with wavelength is quite broad, extending over a >200 nm span. The pump wavelength of 1567 nm and the signal wavelength of 1762 nm are shown with vertical arrows in the plot to illustrate typical operation.

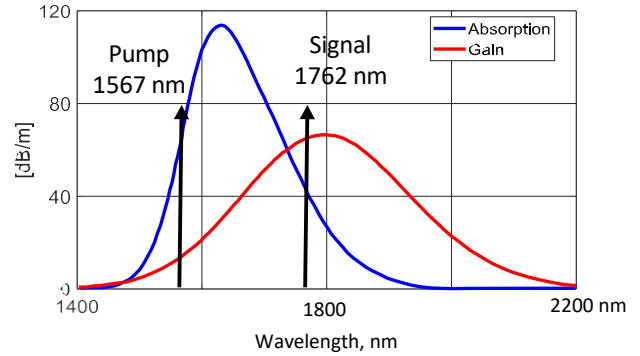


Figure 4. Absorption and gain coefficients as a function of wavelength for the Tm-doped silica fiber.

To complete the theoretical characterization of the fiber, we also need the wavelength independent saturation parameter, the degree of ion pairing present, and the background losses at the pump and signal wavelengths. Values for these parameters are given in [26, 27]. The performance of the Tm-doped fiber is then modeled using two coupled differential propagation and rate equations. Typical accuracy of TDFA simulations is ± 0.5 dB in saturated output power and ± 1 dB in small signal gain.

As an illustration of typical performance of a single-stage TDFA, Figure 5 plots experimental signal output power (blue points) as a function of pump power for an input signal wavelength of 1909 nm and input power of 1 mW (0 dBm). We observe the expected linear dependence of P_{out} with P_{pump} , and a maximum fiber coupled signal output power of 370 mW for a pump power of 2.0 W. The simulated performance of the amplifier, shown with an orange line, agrees well with the experimental data.

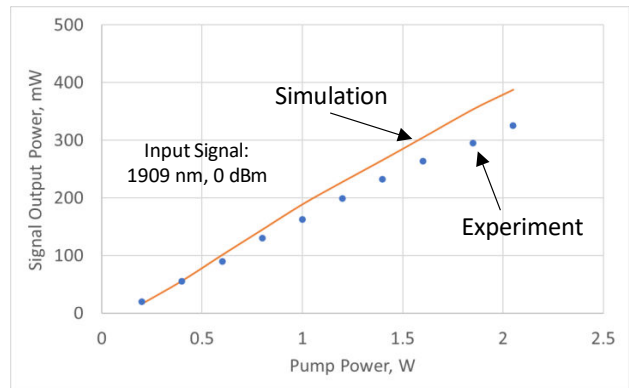


Figure 5. Typical signal output power vs. pump power curve for single stage TDFA

Practical single stage TDFAs are currently limited to output powers of < 1.0 W by the onset of self-lasing as the pump power is increased above the levels used in Figure 5. To achieve stable higher output powers, a two-stage architecture is required. An optimized two-stage architecture and its performance at signal wavelengths between 1760 nm and 1960 nm is the subject of the next section of this paper.

III. DESIGN, OPTICAL ARCHITECTURE, AND PERFORMANCE OF A 1762 nm PM T DFA

Figure 6 shows the optical architecture of a two-stage PM T DFA designed for multi-watt output powers. This amplifier consists of a preamplifier stage followed by a booster stage. A 7-9 W 1567 nm fiber laser pump is split by a 30/70 passive coupler C1 to counter-pump (30%) the preamplifier stage and co-pump (70%) the booster stage via high-power PM fused fiber wavelength division multiplexers WDM1 and WDM2. Both amplifier stages use the same standard commercial 5 μ m core diameter PM TDF (iXblue IXF-TDF-PM-5-125). The gain fibers F1 and F2 are both 1 m long. Optical isolators ISO1-3 establish unidirectional operation and minimize the effects of external reflections on the operation of the fiber amplifier.

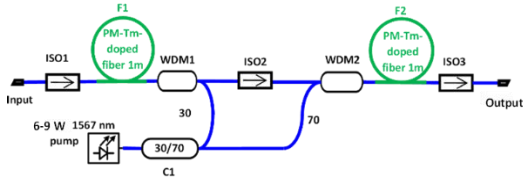


Figure 6. Optical architecture of a two-stage PM T DFA.

As a first example of two stage T DFA performance as a function of wavelength, we show in Figure 7 a plot of the signal output power as a function of signal wavelength for a total pump power of 7 W and an input signal power level of 1 mW (0 dBm). From these data (green points), we see that the experimental output powers are > 2 W over the entire measured signal wavelength range of 1750nm—1910 nm. The simulated output powers, shown in red, agree well with the experimental data. From these measurements, we infer that the 3 dB (50%) output power bandwidth of the T DFA is from < 1750 nm to > 1910 nm.

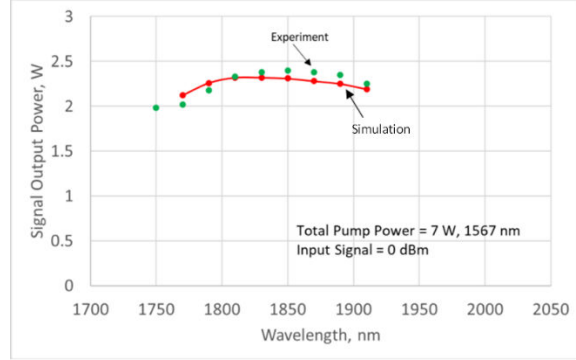


Figure 7. Experimental and simulated output powers for 7 W pump at 1567 nm and 1 mW input signal.

We next increased the pump power to 9 W and also increased the signal input power to 5 mW (+7 dBm). Figure 8 shows the experimental and simulated results for this configuration [27]. Here we measure an experimental output power of 2.95 W at 1760 nm (green asterisk), which agrees well with the simulated output power performance of the amplifier which is shown in red. From this simulated curve, we find that the 3 dB (50%) output power bandwidth of the T DFA is 1745—1980 nm or 235 nm. The simulated external noise figure (blue points) ranges from 7.5 dB to 9.5 dB as expected from theory for this two-stage amplifier design.

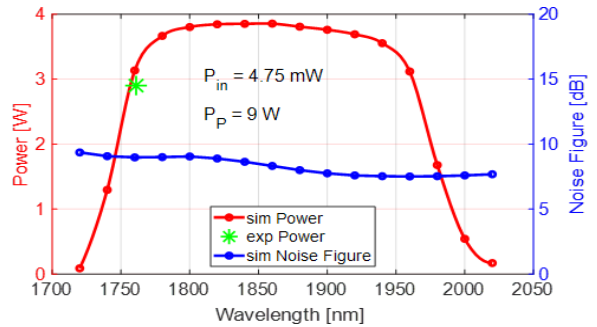


Figure 8. Experimental and simulated output powers for 9 W pump at 1567 nm and 5 mW input signal.

We have also measured the polarization stability and the output power stability of our two-stage TDFA [27]. Figure 9(a) plots the measured polarization extinction ratio (PER) of our fiber amplifier over a time interval of two hours. We find that the PER is > 17 dB as expected from the specifications of the output isolator. The inset in Figure 9(a) shows the typical measured PER contrast curve at a single point in time. Output power stability with time is plotted in Figure 9(b) where we observe a p-p variation of 3.9% and an RMS variation of 0.8% over a time interval of two hours.

The inset in Figure 9(b) shows a photograph of our packaged TDFA. The package dimensions are $200 \times 150 \times 43 \text{ mm}^3$. The amplifier is pumped by a passively cooled semiconductor laser source, has an operating temperature range of -20 to $+40$ C, and is suitable for immediate integration into existing laboratory setups and photonic equipment. The input and output fiber pigtailed are Coherent/Nufern PM1950 fiber cables terminated with FC/APC connectors.

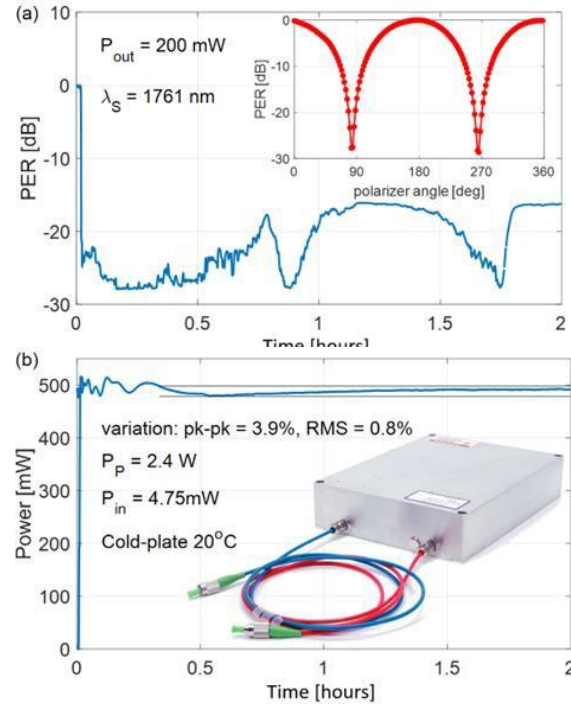


Figure 9.
(a) and (b)

We have additionally experimentally studied the amplification of a single frequency, narrow linewidth (~ 10 kHz) FBG-DFB using a representative TDFA with lower output signal power [28]. Figure 10(a)

shows an experimental setup in which we measured the heterodyne laser linewidth of two single frequency FBG-DFB fiber laser sources. From the experimental heterodyne linewidth plots in Figure 10(b), we find that amplification of 20 dB (100x) in a TDFA has no measurable effect on the 5-10 kHz linewidth of the FBg-DFB fiber laser source. We conclude that the spectral characteristics of a narrow linewidth (5-10 kHz) laser source are not significantly affected by amplification in a representative TDFA.

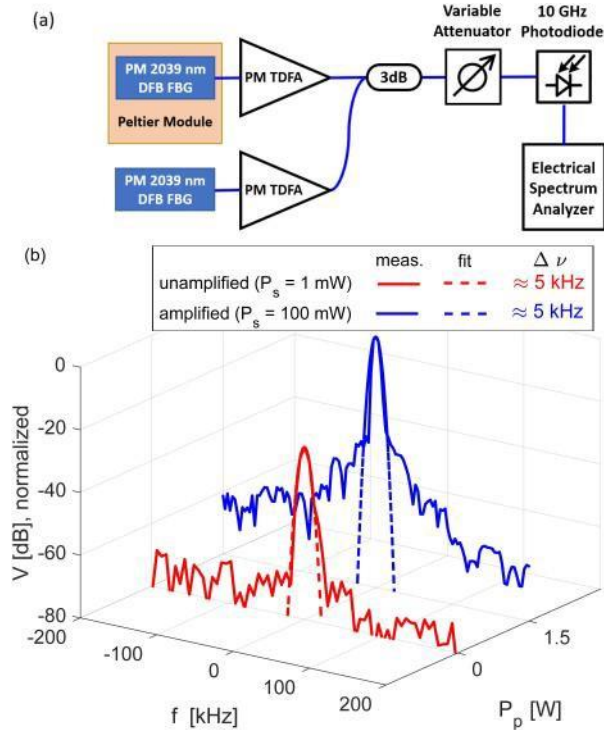


Figure 10. (a) Experimental setup for measuring the heterodyne linewidth of amplified narrow linewidth single frequency fiber laser DFB-FBG sources. (b) Measured heterodyne spectra for unamplified (red) and 20 dB amplified (blue) laser output signals.

Finally we have also measured the pulsed performance of the TDFA [27]. By inserting an A/O amplitude modulator between the preamplifier and the power amplifier stages, we were able to operate the TDFA in pulsed mode. Figure 11 shows examples of the output pulses that we have achieved with 1 and 2 MHz rep rates and 10% duty cycles. For square input pulses, we measured a peaked output pulse as shown in red. We then used an arbitrary waveform generator (AWG) to preshape the input pulse, and obtained the square output pulse shape shown in blue. Peak output

powers of 20 W were achieved in the pulsed operation mode.

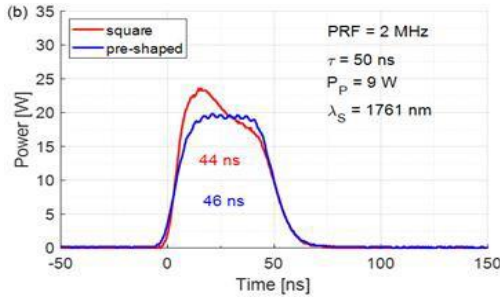


Figure 11. Example of pulsed operation of the 1762 nm two-stage TDFA

IV. APPLICATIONS AND INTEGRATION OF THE 1762 NM TDFA INTO OPTICAL QUBIT EXPERIMENTS USING BA+ IONS

There are many technical and practical advantages in using a fiber coupled single mode TDFA in optical qubit experiments. These include:

- 1) A high Watt-level CW output power of 3W at 1762 nm, at present 6x greater than any other available source.
- 2) Highly stable output power with time.
- 3) The polarization-maintaining operation of the TDFA means that the output polarization state is linear and highly stable. The typical PER is > 17 dB.
- 4) The all fiber design of the TDFA means that no bulk alignment of the components within the optical amplifier is ever required—everything is stable with time.
- 5) The optical modes of the single mode input and output PM optical fibers are Gaussian beams with $M^2 < 1.1$. This means that focusing and collimation of the output laser field are straightforward, with great practical usefulness in experimental optical setups.
- 6) The packaged TDFA is ideal for immediate integration into typical laboratory setups.

As an example of how the TDFA could potentially be applied to enhance and improve a quantum computing measurement, we consider the experimental setup for qubit manipulation at 1762 nm shown schematically in Figure 12 [29].

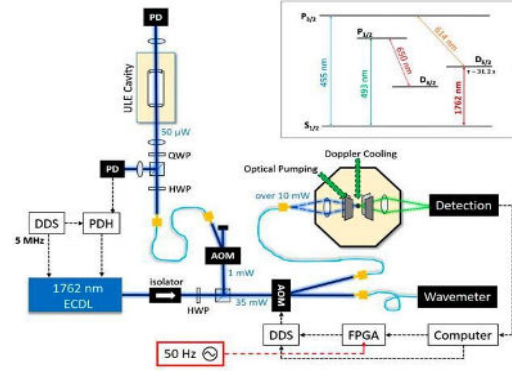


Figure 12. Original experimental setup for qubit manipulation using bulk optics at 1762 nm

Here trapped Ba⁺ ions are used to generate an atomic qubit. In this original experimental setup, the 1762 nm laser signal is generated by an external cavity diode laser (ECDL) using bulk optics and requiring constant alignment for optimum operation. The free space output beam from the ECDL is coupled through a bulk optical isolator followed by free space A/O modulators for frequency stabilization and pulse generation. The free space output beams from the A/O modulators are then focused into single mode optical fibers with significant attendant coupling losses. With this setup, the 1762 nm power available at the input to the ion trap containing the Ba⁺ optical qubits is ~10 mW CW.

Fig. 13 shows a redesigned experimental setup employing an all-fiber single frequency PM FBG-DFB laser at 1762 nm as the source, fiber coupled A/O modulators for pulse generation and frequency stabilization, and the 3W PM TDFA as an optical amplifier after the pulsed A/O modulator. Here polarization-maintaining single mode fibers (shown with a green line) seamlessly interconnect the DFB-FBG laser source, the A/O modulators, and the TDFA with the PDH laser frequency stabilization loop and the ion trap.

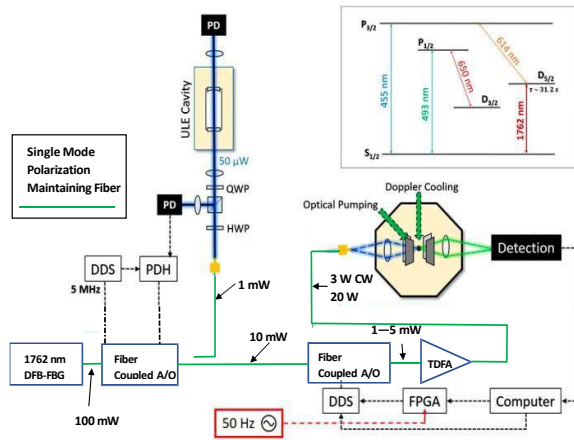


Figure 13. Redesigned optical qubit experiment using all-fiber architecture and a fiber coupled 3 W CW T DFA at 1762 nm.

When the redesigned all-fiber coupled system is run in CW mode, 3 W of stable linearly polarized light is now generated at the input to the ion trap, resulting in a 300x increase in the CW optical power available to the experimentalist. When the system is run in pulsed mode, over 20 W of peak pulsed power (10% duty cycle) is potentially available as well. Also, the former free space bulk optics alignment necessary in Figure 12 for the ECDL, the isolator, the A/O modulators, and the many separated single mode fiber links is now eliminated. This immediately creates a far more stable and user-friendly experimental setup. Overall, the ease and stability of the experimental measurements is greatly improved. With available 1762 nm optical power $\geq 300x$ greater than in the original setup, many new and innovative physics experiments can now be created, designed, and carried out.

We note that the on/off extinction ratio that can be achieved with representative fiber coupled A/O modulators in the 2000 nm band is a minimum of 50 dB and typically 60 dB or greater. This is equivalent to the extinction ratio that can be achieved with free space A/O modulators and that is necessary for high performance quantum computing experiments.

V. DISCUSSION AND CONCLUSIONS

In this paper, we have reported the performance of CW and pulsed single-clad PM Tm-doped fiber amplifiers optimized for the wavelength band from 1760 to 1960 nm. For CW operation, output powers as high as 0.3 W and 3 W were obtained in single- and two-stage amplifier configurations, respectively. The

3 dB (50%) output power bandwidth for the amplifier was 1745–1970 nm or 235 nm. In the pulsed regime, average output powers as high as 20 W were achieved with 50–100 ns pulses.

The wavelength operating band of our T DFA coincides with the 1762 nm infrared transition in Ba⁺ ions, opening up a wide field of experimental applications for this fiber amplifier in optical quantum qubit shelving, manipulation, and control. In a typical laboratory setup, our T DFA could increase the 1762 nm CW optical power available to the quantum experimentalist by a factor of 300x. The increased optical power level will be important for the scaling of quantum computing in applications needing hundreds or even thousands of physical ions to implement basic quantum algorithms using error correction. Using our amplifier as part of an all-fiber architecture also greatly increases the stability and ease of use of the experimental setup. For these reasons, we expect our T DFA to contribute significantly to the next generations of optical qubit experiments and quantum computing experiments using Ba⁺ ions.

VI. ACKNOWLEDGMENT

We are grateful to Ian Farley of Eblana Photonics, Ireland, for the single frequency, narrow linewidth, 1762 nm packaged DML laser source.

VII. REFERENCES

- [1] Nichol, B.C., Srinivas, R., Nadlinger, D.P. et al., “An elementary quantum network of entangled optical atomic clocks”, *Nature* 609, 689–694 (2022). <https://doi.org/10.1038/s41586-022-05088-z>
- [2] M. F. Brandl et al., “Cryogenic setup for trapped ion quantum computing”, *Review of Scientific Instruments* 87, 113103 (2016). <https://doi.org/10.1063/1.4966970>
- [3] Ballance, C., Schäfer, V., Home, J. et al., “Hybrid quantum logic and a test of Bell’s inequality using two different atomic isotopes,” *Nature* 528, 384–386 (2015). <https://doi.org/10.1038/nature16184>
- [4] C. J. Balance, “High-Fidelity Quantum Logic in Ca⁺”, Ph.D. Thesis, Springer International Publishing, 2017. ISBN: 9783319682150, 3319682156.
- [5] Wang, P., Luan, C.Y., Qiao, M. et al., “Single ion qubit with estimated coherence time exceeding one hour,” *Nat Commun* 12, 233 (2021). <https://doi.org/10.1038/s41467-020-20330-w>
- [6] Wright, K., Beck, K.M., Debnath, S. et al., “Benchmarking an 11-qubit quantum computer,” *Nat. Commun.* 10, 5464 (2019). doi: <https://doi.org/10.1038/s41467-019-13534-2>
- [7] George Toh et al., “Progress towards a three-node ion-trap quantum network,” *Proc. SPIE 12446, Quantum Computing, Communication, and Simulation III*, 124460P (8 March 2023); doi: <https://doi.org/10.1117/12.2657155>

- [8] John Hannegan, James D. Siverns, and Qudsia Quraishi, "Entanglement between a trapped ion qubit and a 780-nm photon via quantum frequency conversion," *Phys. Rev. A* 106, 042441 (2022). doi: <https://doi.org/10.1103/PhysRevA.106.042441>
- [9] Alex An Fangzhao, Anthony Ransford, Andrew Schaffer et al., "High fidelity state preparation and measurement of ion hyperfine qubits with $I > \frac{1}{2}$," *Physical Review Letters* 129, 13050 (2022). doi: <https://doi.org/10.1103/PhysRevLett.129.130501>
- [10] Colin D. Bruzewicz, John Chiaverini, Robert McConnell, and Jeremy M. Sage, "Trapped-ion quantum computing: progress and challenges," *Applied Physics Reviews* 6, 02134 (2019). doi: <https://doi.org/10.1063/1.5088164>
- [11] Justin E. Christensen, David Hucul, Wesley C. Campbell, and Eric R. Hudson, "High fidelity manipulation of a qubit built from a synthetic nucleus," *npj Quantum Inf* 6, 35 (2020). doi: <https://doi.org/10.1038/s41534-020-0265-5>
- [12] Justin E. Christensen, "Ba-133: the Goldilocks qubit?," UCLA Hudson Lab for Quantum Interactions and Fundamental Physics (2020). <https://hudsongroup.physics.ucla.edu/cintent/ba-133-goldilocks-qubit>.
- [13] Allison L. Carter, "Design and Construction of a Three-Node Quantum Network," Ph.D. Thesis, University of Maryland, College Park (2021).
- [14] Liudmila A. Zhukas, Peter Svihra, Andrei Nomerotski, and Boris B. Blinov, "High-fidelity simultaneous detection of a trapped-ion qubit register," *Phys. Rev. A* 103, 062614 (2021). doi: <https://doi.org/10.1103/PhysRevA.103.062614>
- [15] Justin Christensen, "High-fidelity operation of a radioactive trapped-ion qubit," Ph.D Thesis, University of California at Los Angeles (2020). <https://escholarship.org/uc/item/1975f05v>.
- [16] Amara A. Graps, "From Perfect Qubit to Goldilocks Qubit for Ion Traps," <https://www.insidequantumtechnology.com/news-archive/from-perfect-qubit-to-goldilocks-qubit-for-ion-traps/>
- [17] Eblana Photonics EP1762-2-DM-B06-FM, <https://cyberllc.com/wp-content/uploads/2021/05/EP1742-DM-B.pdf>
- [18] Dutta, T., "An injection-locked 1762 nm laser for trapped barium ion qubits," *Appl. Phys. B* 128, 136 (2022). <https://doi.org/10.1007/s00340-022-07838-3>
- [19] M. R. Dietrich, A. Avril, R. Bowler, N. Kurz, J. S. Salacka, G. Shu, and B. B. Blinov, "Barium Ions for Quantum Computation," *AIP Conference Proceedings* 1114, 25 (2009); <https://doi.org/10.1063/1.3122286>
- [20] NKT Photonics, Koheras Adjustik Fiber Laser at 1762 nm (2023), <https://www.nktphotonics.com/products/single-frequency-fiber-lasers/koheras-adjustik/>
- [21] M. Nakazawa, K. Suzuki, and Y. Kimura: *Proc. Int. Conf. Integrated Optics and Optical Fiber Communication (IOOC 1989)*, Vol. 3, p. 28.
- [22] Y. Kimura, K. Suzuki, and M. Nakazawa: *Proc. Int. Conf. Integrated Optics and Optical Fiber Communication (IOOC 1989)*, Vol. 3, p. 38.
- [23] D. Richardson, Tutorial W4E.1, OFC 2022
- [24] P. C. Becker, N. A. Olsson, and J. R. Simpson, "Erbium-Doped Fiber Amplifiers: Fundamentals and Technology," Academic Press, New York, 1999. ISBN: 0-12-084590-3
- [25] D. Derickson, "Fiber Optic Test and Measurement," Prentice-Hall, Upper Saddle River, NJ (1998). ISBN 0-13-534330-5
- [26] C. Romano, R. E. Tench, and J.-M. Delavaux, "Simulation of 2 μ m single clad thulium-doped silica fiber amplifiers by characterization of the 3F4–3H6 transition," *Opt. Express*, vol 26, no. 20, pp. 26080–26092, Oct. 2018. <https://doi.org/10.1364/OE.26.026080>
- [27] W. Walasik, R. E. Tench, G. Rivas, J. Delavaux, and I. Farley, "1760 nm Multi-Watt Broadband PM CW and Pulsed Tm-doped Fibre Amplifier," in *European Conference on Optical Communication (ECOC) 2022*, J. Leuthold, C. Harder, B. Offrein, and H. Limberger, eds., Technical Digest Series (Optica Publishing Group, 2022), paper Th2A.3. ISBN: 978-1-957171-15-9
- [28] Wiktor Walasik, Daniya Traoré, Alexandre Amavigan, Robert E. Tench, Jean-Marc Delavaux, and Emmanuel Pinsard, "2- μ m Narrow Linewidth All-Fiber DFB Fiber Bragg Grating Lasers for Ho- and Tm-Doped Fiber-Amplifier Applications," *J. Lightwave Technol.* 39, 5096-5102 (2021). <https://doi.org/10.1109/JLT.2021.3079235>
- [29] Dahyun Yum, Debashis De Munshi, Tarun Dutta, and Manas Mukherjee, "Optical barium ion qubit," *J. Opt. Soc. Am. B* 34, 1632-1636 (2017) <https://doi.org/10.1364/JOSAB.34.001632>